Proceedings of the 15th International Symposium on the Packaging and Transportation of Radioactive Materials
PATRAM 2007
October 21-26, 2007, Miami, Florida, USA

NATURAL CONVECTION/RADIATION HEAT TRANSFER SIMULATIONS WITHIN THE FUEL REGIONS OF A TRUCK CASK UNDER 10CFR71-FORMAT FIRE CONDITIONS

Venkata V.R. Venigalla
Research Assistant
Mechanical Engineering Department
University of Nevada Reno
Reno, Nevada 89557
venkata.venigalla@gmail.com

Miles Greiner
Professor of Mechanical Engineering
University of Nevada, Reno
Reno, NV 89557
Phone-(775) 784-4873
greiner@unr.edu

ABSTRACT

Light water reactor nuclear fuel assemblies consist primarily of fuel rods held in square arrays by periodic spacer plates. The rods consist of heat-generating spent fuel pellets within zircaloy cladding. Spent fuel is transported away from reactors in thick wall casks. Individual assemblies are supported in square cross-section basket openings that are filled with non-oxidizing gas. Risk analysts must determine the fuel cladding temperature during and after events in which the cask is engulfed in large, long duration fires. Finite element cask models are used for that purpose. Those models typically employ Effective Thermal Conductivities (ETC) in the fuel regions. These ETC's have been developed to model heat transfer for normal conditions of transport. However, they have not been shown to be conservative for the high temperature and transient conditions that are caused by fires.

In the current work, a two-dimensional cross section model of a Legal Weight Truck (LWT) package, designed for four Pressurized Water Reactor (PWR) assemblies, is developed. Each PWR assembly consists of a 15x15 square array of heat-generating fuel rods. The Fluent computational fluid dynamics (CFD) package models three processes: 1) buoyancy-induced gas motion within the fuel regions; 2) the convective/radiation heat transfer within the fuel regions; and 3) the conduction in the solid regions. These simulations are used to determine the fuel cladding temperature during and after 10CFR71 regulatory format fires with different durations. They are also used to determine the minimum fire durations that bring the fuel cladding to its initial creep deformation and its burst rupture temperatures. The results are compared to those from finite element models that employ ETC's in the fuel regions.

INTRODUCTION

The goal of this work is to develop computational tools to predict the temperature of spent nuclear fuel cladding in transport casks during severe fire events. Light water reactor nuclear fuel assemblies consist of fuel rods held in square arrays by periodic spacer plates [1, 2]. The rods themselves are stacks of UO_2 fuel pellets within zircaloy cladding. Some spaces in the array contain hollow instrumentation or guide thimble tubes instead of fuel rods. Boiling water reactor (BWR) fuel assemblies consist of 6×6 to 9×9 arrays of rods surrounded by a square-

cross-section zircaloy channel. Pressurized water reactor (PWR) assemblies generally consist of 9x9 to 17x17 rod arrays but do not have surrounding channels. PWR rod diameters are generally smaller than those of BWRs, but they have larger total assembly cross sections.

Spent nuclear fuel (SNF) is placed in water pools after it is removed from a reactor to allow its heat generation and radioactive decay rates to decrease [3]. After an appropriate time, SNF is placed in casks for dry storage or offsite transport [4, 5]. In transportation casks, individual SNF assemblies are supported horizontally within square cross-section openings of a basket structure inside the cask's containment region. That region is evacuated and backfilled with helium or another non-oxidizing gas. Casks transported by truck have enough space for roughly 4 PWR assemblies, while those transported by rail hold around 21 assemblies [4, 5].

Federal regulations require casks that transport large quantities of radioactive materials (Type B packages) be analyzed in a 38^{o}C environment for normal transport and in an 800^{o}C fire environment for duration of 30 minutes for accident conditions [6]. Fuel cladding encapsulating the UO_2 pellets provides an important containment boundary. During normal transport the fuel cladding temperature must not exceed 400^{o}C [7].During a fire the fuel cladding may experience creep deformation if its temperature exceed 570ºC, or burst rupture if it exceed 750ºC [8, 9]. There is therefore a need to accurately predict the fuel cladding temperatures during various conditions that may occur during transportation.

The thermal performance of packages for regulatory testing and other severe events is evaluated by both testing and analysis. Analyses typically involve construction of finite element thermal models of intact or damaged packages. First the steady state package temperatures are calculated for a normal transport environment. These temperatures are used as initial conditions for a transient calculation that determines the time-dependent package temperatures during a fire. Finally, the package temperatures at the end of the fire are used as initial conditions for a post-fire cool down calculation.

The multiple fuel regions within a cask are difficult to model because each contains many fuel rods. In the past, computational resources were not available to perform calculations using models that accurately represented the fuel. To address this problem, the fuel assemblies and backfill gas were replaced by fictitious but representative solid elements with temperature-dependent Effective Thermal Conductivities (ETC) [2, 4, 10 and 11].

Manteufel and Todreas [11] developed ETCs based on a one-dimensional analytical model of radiation and conduction heat transfer in a two-dimensional array of heated rods within a stagnant gas. That model does not account for natural convection, unheated tubes or channels, or multi-dimensional effects. Bahney and Lotz [2] performed two-dimensional finite element thermal simulations of several different fuel assemblies, including unheated components, within isothermal enclosures. They developed ETCs based on conduction and radiation heat transfer. In some cases, ETC models are employed in analysis without stating their source or the methods used to develop them [4, 10].

Greiner et al. [12] used ETC models to estimate the temperature within a rail cask for normal transport. Multiple simulations were performed using two different ETC models in a two-dimensional finite element model of a cask capable of carrying 21 PWR fuel assemblies. They determined the cask Thermal Dissipation Capacity Q_{TDC}, which is the heat generation that brings the fuel cladding to the maximum allowable limit of 400^{o}C for normal transport. They also determined that the support basket wall temperatures in the periphery of the package are highly non-uniform.

Venigalla et al. [13] performed two-dimensional thermal simulations of a truck cask designed to transport four PWR assemblies. The model included 15x15 arrays of fuel rods within four square cross section openings that support the fuel. Computational fluid dynamics (CFD) simulations calculated buoyancy induced motion within, and natural convection and

radiation heat transfer across, the gas filled regions. Stagnant-gas CFD (S-CFD) simulations, with zero gas speed, were compared to the CFD results to evaluate the effect of gas motion. Simulations using ETCs in the fuel region were performed for comparison. Simulations were performed for helium (He) and nitrogen (N_2) cover gases. The value of Q_{TDC} predicted by CFD and S-CFD models were nearly identical. This indicates that gas motion does not significantly affect heat transfer. The value of Q_{TDC} predicted by ETC was 6% lower than that predicted by CFD. Gudipati et al. [14] applied the thermal simulation techniques developed for a truck cask by Venigalla et al. [13] to a much larger rail cask. For a large rail cask Q_{TDC} predicted by S-CFD calculations is essentially the same as that predicted by the CFD simulation, and both are 3-6% higher than that predicted by the ETC model. ETC models over predict cladding temperatures during normal transport because they neglect certain heat transfer effects.

ETC's have also been used to predict the peak cladding temperature during fire accident conditions [15-18]. However since ETC models neglect some thermal effects, they may under predict the heat transfer to the fuel from a fire and the resulting fuel clad temperatures. ETC models have not been shown to be conservative for fire accident conditions.

In the current work, geometrically accurate two-dimensional models of a Legal Weight Truck (LWT) cask cross-section developed by Venigalla et al. in [13] is used. Four PWR assemblies, each consisting of a 15x15 square array of heat generating fuel rods, are placed within the basket openings. The Fluent CFD package models the buoyancy-induced gas motion and natural convection/radiation heat transfer within the fuel regions, as well as conduction in the solid regions. This model is subjected to the regulatory format fire model (fully engulfing, 800°C regulatory fire with a range of fire durations). The fire durations that bring the fuel cladding temperature to its initial creep deformation temperature and to its burst rupture temperature are determined. The results are compared to those from S-CFD and ETC fuel region models.

COMPUTATIONAL MODEL

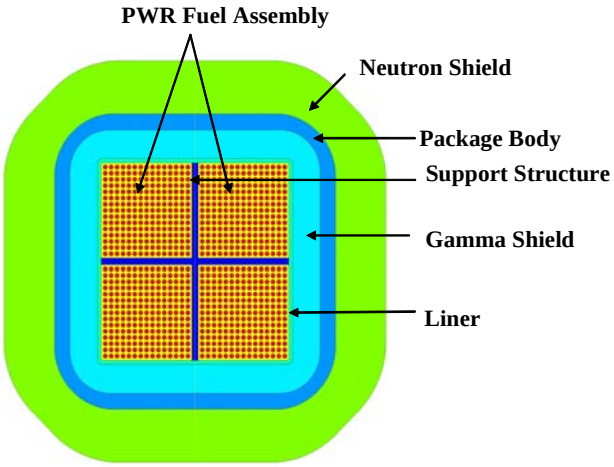

Figure 1: Cross section of a Legal Weight Truck (LWT) cask that transports four spent pressurized water reactor fuel assemblies.

Figure 1 shows the cross section of a LWT cask package used in the current analysis. It is similar but not identical to the currently licensed cask [4]. The cross section in Fig. 1 is midway between cask ends. The dot-filled region represents four 15x15 PWR fuel assemblies within backfill gas. All 225 fuel rods of each assembly are identical. Each contains UO_2 pellets of diameter 9.36 mm enclosed in zircaloy cladding of thickness 0.78 mm. No gap or contact resistance between the pellets and cladding are modeled. The tube array has center to center

spacing of 14.5 mm, and the distance between the center of the outer most rod and the basket wall is 9.82 mm. The fuel assembly is similar to a Babcock & Wilcox 15x15 Mark B PWR, but the model does not contain unheated components.

The cross-shaped component at the center of the package is a 1.5 cm thick stainless steel support structure. Its surface emissivity is 0.8. Borated carbon (B_4C) pellets fill 1.1 cm-diameter holes that are drilled radially in the legs of the structure. The sides of the four square openings where the fuel is placed are 22.3 cm long.

The support structure and fuel are surrounded by a 0.96 cm thick stainless steel liner. Its emissivity is 0.2. The liner is surrounded by a depleted uranium gamma shield. Its maximum thickness is 6.7 cm and it has an outer radius of curvature of 11.4 cm at its corners. A 3.8 cm thick stainless steel package body surrounds the gamma shield.

An external, 12.4-cm-thick neutron shield encircles the package. A single region is used to model several components. These components are 12.1-cm-thick Polypropylene-1% boron, 24 aluminum radial fins of thickness 0.245 cm, and a 0.27 cm thick stainless steel outer skin. The mixture thermal conductivity for this composite structure was developed based on an equivalent conduction model [17].

Figure 2 shows the computational mesh used in the current work. Only one half of the cask cross section is modeled to take advantage of the geometric and boundary condition symmetry. The computational grid was constructed using MSC Patran software. The dimensions and gaps utilized in the current model are described in [13].The current simulations calculate the cask and fuel temperatures using three different fuel region models. One model uses CFD simulations that include buoyancy-induced fluid motion. Another uses CFD but assumes the gas speed is zero (Stagnant-CFD or S-CFD). Both these models include the effects of radiation heat transfer across the gas-filled regions. Comparison of these two results shows the effect of gas motion. The last model employs the ETC's developed by Manteufel and Todreas [11]. Mesh independency was verified in the previous work using two different grid sizes [13].

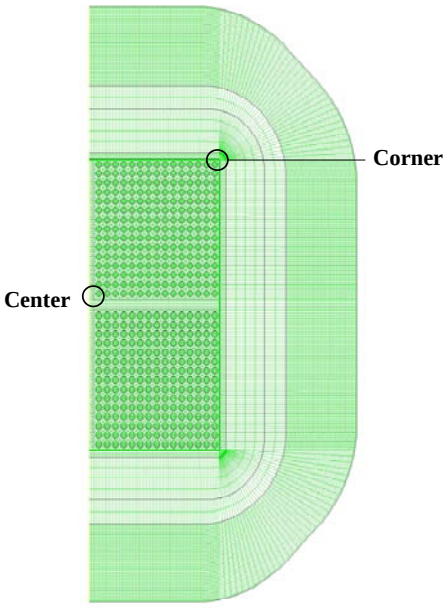

Figure 2: Computational domain of a LWT cask with 46798 elements.

The ETC simulations are performed using the Patran P/thermal finite element code. The model by Manteufel and Todreas [11] is applied to the 15x15 PWR assembly used in the current work. In that model the region inside each square opening of the fuel basket is divided into a

21.7 cm x 21.7 cm central square that represents the fuel assembly, and a 0.3 cm thick edge region that represents the gas-filled gap between the assembly and basket. The model by Manteufel and Todreas [11] gives two different temperature dependent conductivities for the interior and edge regions k_{INT} and k_{EDGE} as shown in Figure 3. A detailed description of the cask geometry, computational domain, and ETC model is presented in [13].

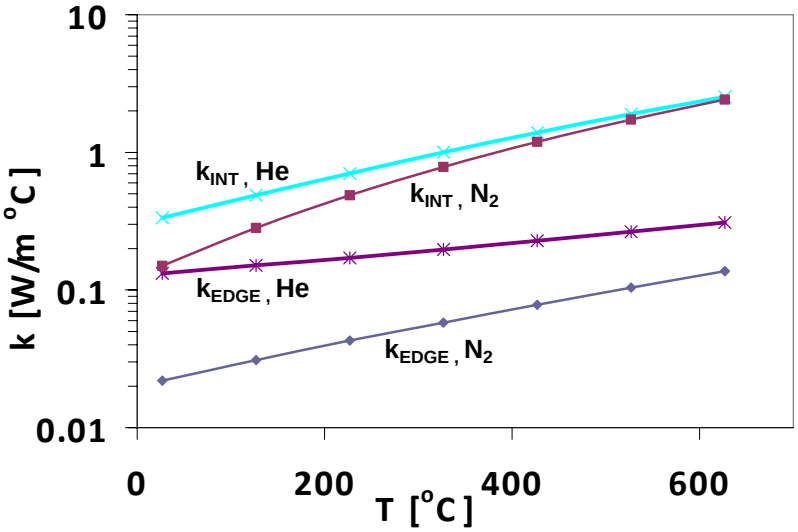

Figure 3: Effective thermal conductivity versus Temperature for Helium and Nitrogen backfill gases.

CASK BOUNDARY CONDITIONS

The steady state package temperatures were calculated for the regulatory normal transport environment in [6, 13]. These temperatures are used as initial conditions for a transient calculation that determines the time-dependent package temperatures during a fire. Finally, the package temperatures at the end of the fire are used as initial conditions for a post-fire cool down calculation. A detailed description of the cask boundary conditions for normal transport can be found in [13]. During the fire the bulk temperature and pressure of the gas contained in the fuel region both increase. However, since the mass and the volume are constant the density is constant. The current simulations assume the pressure does not change. Future work may consider the effect of variable pressure.

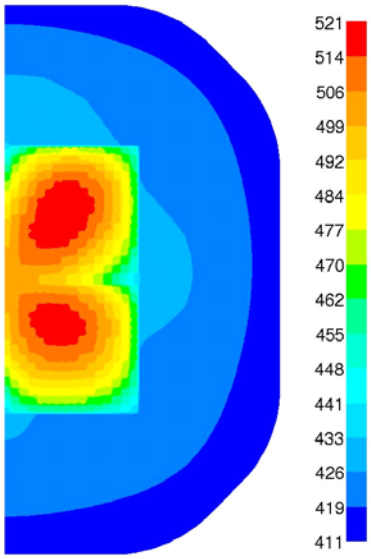

Figure 4: Normal hot day transport temperature contours (in Kelvin) with 800W/assembly using CFD model, N_2 Backfill.

Pre-Fire Simulations.

At an assembly heat generation rate of Q=800 W/assembly each model gave different initial peak clad temperature. Future work will consider different Q's for each models so that they all have the same initial peak clad temperature. Figure 4 presents the temperature contours for CFD simulation with N_2 in the backfill region.

Fire/Post-Fire Simulations.

The normal conditions of transport temperatures described in [13] are used as initial conditions (time t = 0) for the transient fire simulations. The Code of Federal Regulations (10CFR71) specifies a fire heat transfer model that consists of a fully-engulfing fire temperature and emissivity of at least 800°C and 0.9, and appropriate convection [9]. For the current fire simulations, these lower limits are used along with a package surface emissivity of 0.8. For simplicity's sake, convection heat transfer between the fire and package is not included (The sensitivity of the results to convection can be considered in future work). The 10CFR71 regulations specify a fire duration of D = 0.5 hr. In the current work, we calculate the package response for a range of fire durations.

The package temperatures at the end of the fire (time t = D) are used as the initial condition for a transient post-fire calculation. In this work, the post-fire environment is identical to the normal hot day transport conditions. These simulations calculate the temperatures throughout the package after the fire.

RESULTS AND DISCUSSIONS

Transient Response, D = 0.5 hr, N_2

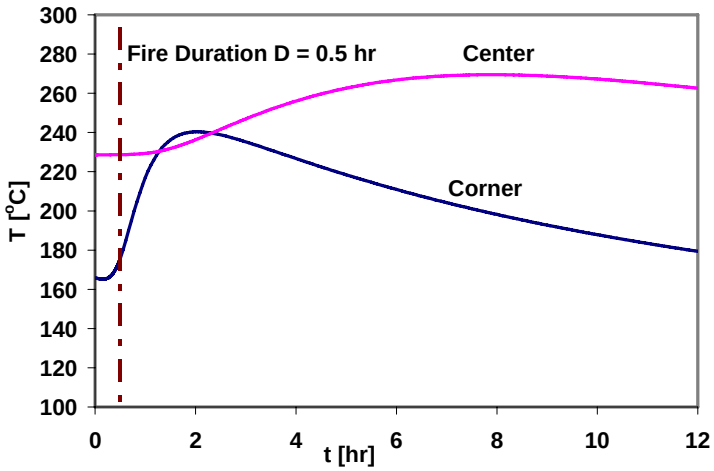

Figure 5: Center and Corner Fuel Temperature versus Time for a CFD simulation with N_2 gas for a fire duration of 30 minutes.

Figure 5 shows the temperature response versus time of the fuel cladding at the center and corner locations in the upper fuel assembly in Figure 2 for a 30-minute fire. They are the only two locations where the cladding temperature is monitored in this work. A vertical dashed line shows the time at which the simulated fire ends and the post-fire conditions begin. The cladding temperatures at center and corner begin to rise after the fire begins. They continue to rise after the fire is extinguished before peaking and then slowly decreasing. This delay is due to heat continuing to diffuse to the fuel from the hotter regions in the periphery of the cask. The fuel cladding corner temperature rises sooner compared to the center because it is closer to the

exterior surface heated by fire. However, the center exhibits the maximum temperature in the fuel region. For a 30-minute regulatory fire with N_2 backfill, the peak post-fire temperature is 269°C.

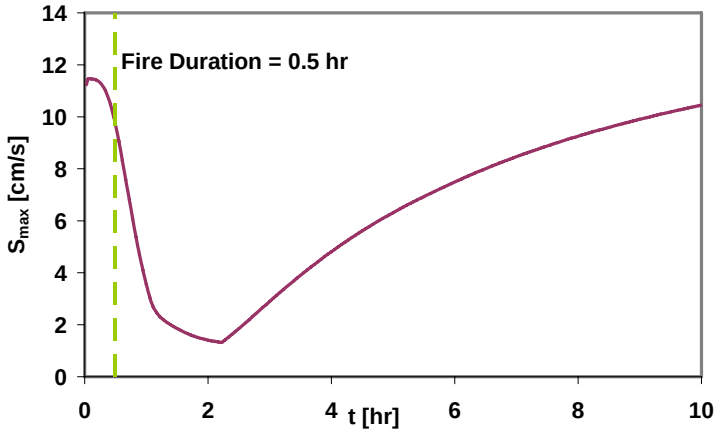

Figure 6: Maximum Gas Speed versus Time for D=30 min, N_2 cover gas

Figure 6 shows the maximum gas speed versus time in the fuel regions for N_2. Buoyancy effects in the backfill gas affect the velocity. The gas speed decreases for the first 2 hours as the temperature difference between center and corner fuel decreases (See Figure 5). After t=2 hours the fuel regions start losing heat, the temperature gradients in the fuel regions increase, thereby causing increased buoyancy in the backfill gas. This can be seen in that the gas velocities start increasing at approximately 2 hrs. The speeds in Figure 6 and temperatures in Figure 5 approach their pre-fire conditions after t=10 hours.

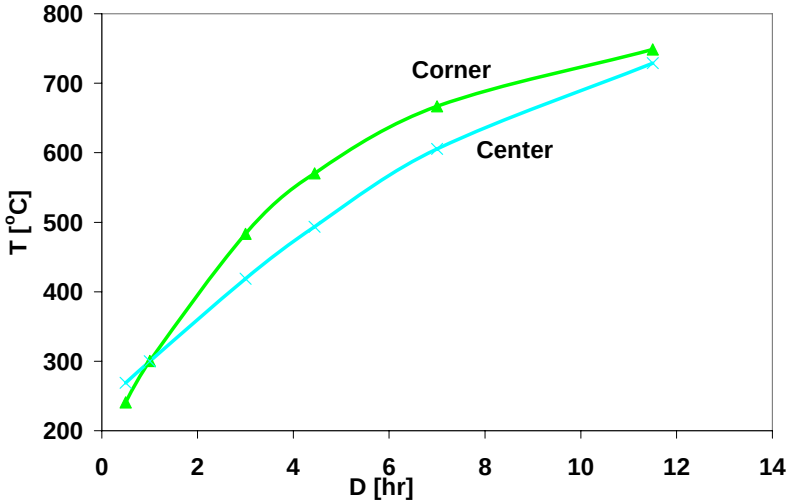

Figure 7: Maximum Center and Corner Temperature vs. Fire Duration for CFD simulations for N_2

Figure 7 presents the maximum temperatures attained at the center and corner locations for a range of fire durations D, for N_2 backfill gas. For short durations, the maximum center temperature is greater than the maximum value at the corner. This is because the fire does not last long enough to cause the temperature profile shape to deviate far from its initial conditions. For intermediate duration fires (1 hour < D < 12 hour) the maximum corner temperature is hotter

than that at the center. Visual extrapolation of the data in Figure 7 suggests that for longer fire durations, i.e. D > 12, hrs, the maximum center temperature is greater than that at the corner. This may be because the temperature profiles approach steady state when the fire lasts for very long periods.

Figure 8 shows the Peak Fuel Clad temperature in the post-fire period as a function of fire duration from CFD, S-CFD, and ETC simulations. The Peak Fuel Clad temperature is the larger of the maximum at the center and corner. The true peak temperature for the domain may be at some other locations but these were the only two locations that were monitored in this work. Horizontal lines show the cladding temperatures of concern for creep deformation, T_{CD} = 570°C [8] and burst rupture temperature T_{BR} = 750°C [9].

In Figure 8 it can be seen that 1) the peak fuel cladding temperatures increases with fire duration; and 2) the values for the three different fuel region models diverge with increasing fire duration. For short duration fires (D<2hr), the ETC model predicted the hottest fuel cladding temperatures, for 2hr < D < 5.5hr the CFD simulations predicted higher temperatures compared to ETC. For D > 5.5hr the S-CFD simulations predicted the highest peak temperatures. Some of the differences between the simulations may be due to the limited number of locations where the fuel is monitored or because the initial pre-fire temperature for the three models is not the same.

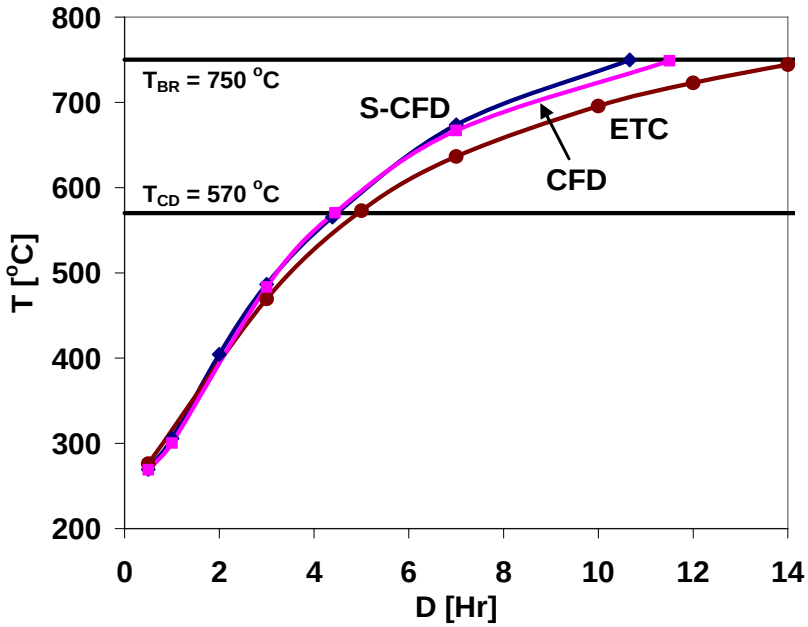

Figure 8: Peak Cladd Temperatures caused by Fires with various Durations calculated by CFD, S-CFD and ETC for N_2

	N_2		He	
Fuel Model	$D_{C,CD}$ [hr]	$D_{C,BR}$ [hr]	$D_{C,CD}$ [hr]	$D_{C,BR}$ [hr]
ETC	5	14	4.7	14
S-CFD	4.39	10.66	4.22	10.66
CFD	4.44	11.5	4.39	11.33

Table-1: Durations of Concern for Fuel Clad based on Creep Deformation and Burst Rupture for He and N_2 from all the fuel models.

The fire durations that cause the cladding to reach the long-term creep deformation temperature and burst rupture temperatures, T_{CD} and T_{BR} are denoted $D_{C,CD}$ and $D_{C,BR}$, respectively. They are the durations at which the peak cladding temperature curves in Figure 8 cross the horizontal lines for these temperatures. Table 1 summarizes $D_{C,BR}$ and $D_{C,CD}$ from all three models and both cover gases.

Table 1 shows that the durations of concern for helium are nearly the same or slightly shorter than they are for nitrogen. Moreover, the duration of concern for burst rupture is 2.4 to 3 times longer than they are for creep deformation. A comparison of duration of concern between various models from Table 1 shows that the time for creep deformation, DC,CD is 11 % lower for CFD in comparison with ETC and that the time for burst rupture, DC,BR is 24 % lower for CFD in comparison with ETC model.

CONCLUSIONS

This work assesses the temperature response and resulting containment integrity of the fuel cladding within a generic legal weight truck package during and after regulatory format fires using different fuel region models. The package studied in this work resembles a modern cask designed to transport four PWR fuel assemblies. This work uses a two-dimensional finite volume mesh that accurately represents the geometry of a legal weight truck cask, including the fuel inside the cask. CFD simulations are performed that calculate buoyancy-driven gas motion, as well as the natural convection and radiation heat transfer in the gas filled fuel region. Simulations are also conducted without the buoyancy-driven gas motion and with accurate fuel geometry.

The package steady state temperatures are determined for normal hot day transport conditions. These temperatures are used as the initial conditions for fully-engulfing fire simulations with an effective temperature of 800°C and emissivity of 0.9. Although the duration of the 10CFR71 regulatory fire is 0.5 hr, simulations in this work are performed for a range of durations. The package temperatures at the end of the fire are used as the initial conditions for post-fire cool down simulations. The maximum fuel cladding temperatures are determined for a range of fire durations. The temperatures of the fuel cladding closest to and farthest from the cask center are monitored during and after the fire.

The fuel cladding is an important containment boundary for spent fuel. For all three fuel region models, the minimum fire durations that cause the cladding to reach its initial creep deformation temperature and its burst rupture temperature are determined. CFD simulations predict higher peak cladding temperatures the ETC calculations. As a result, CFD simulations predict that shorter duration fires will cause the cladding to reach temperatures of concern than are predicted by ETC calculations. This suggests that ETC models may not be conservative for calculating the response of fuel cladding during fire accident conditions. Future simulation must be performed that monitor the cladding temperature at more locations, and consider a range of fuel heat generation rates, to more accurately compare the predictions from CFD and ETC fuel models.

ACKNOWLEDGMENTS

This work was sponsored by the US Global Nuclear Energy Partnership (GNEP) under contract DE-FC07-06ID14782.

REFERENCES

[1] U.S Department of Energy, 1987, “Characteristics of Spent Nuclear Fuel, High-Level Waste, and Other Radioactive Wastes Which May Require Long-Term Isolation”, Office of Civilian Radioactive Waste Management, DOE/RW-0184.

[2] Bahney, R.H., and Lotz, T.L., 1996, “Spent Nuclear Fuel Effective Thermal Conductivity Report,” prepared for the U.S. DOE, Yucca Mountain Site Characterization Project Office by TRW Environmental Safety Systems, Inc., D.I.: BBA000000-01717-5705-00010 REV 00.

[3] Saling, J.H. and Fentiman, A.W., 2001, *Radioactive Waste Management*, 2nd Edition, Taylor and Francis, New York.

[4] General Atomics (GA), 1998, “GA-4 Legal Weight Truck From-Reactor Spent Fuel Shipping Cask, Safety Analysis Report for Packaging (SARP),” San Diego, California 92186-5608.

[5] Office of Civilian Radioactive Waste Management (OCRWM), US Department of Energy, 1993, “Multi-Purpose Canister (MPC) Implementation Program Conceptual Design Phase Report,” DOC ID: A20000000-00811.

[6] U.S. Nuclear Regulatory Commission, “Packaging and Transportation of Radioactive Material,” Rules and Regulations, Title 10, Part 71, Code of Federal Regulations.

[7] Nuclear Regulatory Commission (NRC), 2005, “Cladding Considerations for the Transportation and Storage of Spent Fuel”, Interim Staff Guidance Report for the Spent Fuel Project Office of the U.S., ISG-11 Rev. 3, available at www.nrc.gov

[8] Johnson, A.B. and Gilbert, E.R., September 1983, “Technical Basis for Storage of Zircaloy-Clad spent Fuel in Inert Gases,” PNL-4835, Pacific Northwest Laboratory, Richland, Washington.

[9] Sprung, J.L., Ammerman, D.J., Breivik, N.L., Dukart R.J. and Kanipe, F.L., March 2000, “Reexamination of Spent Fuel Shipment Risk Estimates, NUREG/CR-6672, Vol.1 (SAND2000-0234), Sandia National Laboratories, Albuquerque, New Mexico.

[10] Unterzuber, R., Milnes, R.D., Marinkovich, B.A. and Kubancsek, G.M., 1982, “Spent-Fuel Dry-Storage Testing at EMAD (March 1978 through March 1982),” Prepared for the US DOE Commercial Spent Fuel Management Program Office at the Pacific Northwest Laboratory, B-D3339-A-G.

[11] Manteufel, R.D., and Todreas, N.E., 1994, “Effective thermal conductivity and edge conductance model for a spent fuel assembly,” *Nuclear Technology*, Vol. 105, pp. 421-440.

[12] Greiner, M., Gangadharan, K.K., and Gudipati, M. , 2006, "Use Of Fuel Assembly/Backfill Gas Effective Thermal Conductivity Models to Predict Basket and Fuel Cladding Temperatures within a Rail Package during Normal Transport," PVP2006-ICPVT-11-93742, *Proceedings of ASME Pressure Vessels and Piping Division Conference*, July 23-27, Vancouver, BC, Canada, to appear *Nuclear Technology*, 2007.

[13] Venigalla, V.V.R., and Greiner, M., 2007, “CFD Simulations of Natural Convection/Radiation Heat Transfer within the Fuel regions of a Truck Cask for Normal Transport," PVP2007-26242, *Proceedings of the 2007 ASME Pressure Vessels and Piping Division Conference*, July 22-26, 2007, San Antonio, Texas.

[14] Gudipati, M., and Greiner, M., 2007, "CFD Simulations of Fuel Cladding and Basket Surface Temperatures in an MPC Rail Cask during Normal Transport," *Proceedings of*

the 15th International Symposium on the Packaging and Transportation of Radioactive Materials (PATRAM).

[15] Greiner, M., S. Shin, R.J. Faulkner and R.A. Wirtz, 1998a, “Transport Cask Response to Regulatory Format Thermal Events, Part 1: Rail Package,” *International J. of Radioactive Material Transport*, Vol. 9, n 3, pp. 187–192.

[16] Greiner, M., R.J Faulkner and Y.Y. Jin, 1998b, “Transport Cask Response to Regulatory Format Thermal Events, Part 2: Truck Cask,” *International J. of Radioactive Material Transport*, Vol. 9, n 3, pp. 193–198.

[17] Mallidi, N., Greiner, M., and Venigalla, V.R.V., 2006, "Fire Durations of Concern for a Modern Legal Weight Truck Cask," PVP2006-ICPVT-11-93748, *Proceedings of ASME Pressure Vessels and Piping Division Conference*, July 23-27, Vancouver, BC, Canada.

[18] Adkins, H.E. Jr., Cuta, J.M., Koeppel, B.J., Guzman, A.D., and Bajwa, C.S., 2006, “Spent Fuel Transportation Package Response to the Baltimore Tunnel Fire Scenario,” NUREG/CR-6886, Rev. 1, PNNL-15313, Pacific Northwest National Laboratory.